Synthesis, Charecterization, Antibacterial and Cytotoxicity of Novel Metal Complexes Derived from Azomethine Ligand (Bis Azo-Schiff Base) *In Vitro* and *In Silico*

Hussein Abdulkadhim Hasan [1*], Saad M. Mahdi [1], Hanaa Addai Ali [2]

Abstract

Background: Schiff bases, especially Azo-Schiff bases, are significant ligands in organic chemistry due to their coordination capabilities. They find applications in various industrial sectors and biological studies. Metal complexes of Schiff bases, particularly with tetradentate ligands, have gained attention for their potential pharmacological benefits. However, there is limited information on the biological activities of certain Schiff base complexes, such as 1H-indole-3-ethylenesalicyldamine derivatives. Method: The synthesis of bis azo-Schiff base ligands and their metal complexes, including Ni(II), Co(II), Pd(II), and Pt(IV) complexes, was conducted. Various analytical techniques were employed to characterize the compounds using FTIR, NMR, UV-Vis spectroscopy, mass spectrometry, and molar conductivity. Biological activities, including antibacterial and cytotoxicity studies, were evaluated. Results: The synthesized compounds demonstrated stability and structural characteristics consistent with the intended coordination geometries. IR spectra confirmed the coordination of metal ions with the ligands. The complexes were evaluated for the antimicrobial activity against two types strains of Gram-negative Escherichia coli and Gram-positive bacteria Staphylococcus aureus and showed good significant against these bacteria. The Pd(II) complex demonstrated higher efficacy against cancer cells compared to normal cells, highlighting its potential as an anticancer agent. The cytotoxicity of the Pd (II) complex on human malignant melanoma A375 and Normal cell WRL-68 were IC50 23.83 and IC50 153.7, respectively. Molecular docking studies provide insights into the interaction of the complexes with target proteins, offering potential modes of action. Conclusion: The study successfully synthesized and characterized bis azo-Schiff base ligands and their metal complexes, demonstrating their stability and promising biological activities.

Keywords: Azo dye, Antibacterial, A375 cell line, Molecular docking, Complexes of Ni(II), Pd(II), and Pt(II), Schiff base.

Significance | This study demonstrated the synthesis of Schiff bases, like azo-Schiff metal complexes, showing therapeutic effects.

*Correspondence. Hussein Abdulkadhim Hasan, Department of Chemistry, College of Science, University of Babylon, Babylon, Iraq.
E-mail: huss17ein@gmail.com

Editor Aman Shah Bin Abdul Majid And accepted by the Editorial Board Mar 10, 2024 (received for review Jan 4, 2024)

Introduction

Schiff bases are widely recognized for their coordination capabilities, making them one of the most significant ligands in contemporary organic chemistry (Dalaf et al., 2018). Azo-Schiff bases, which have imine groups (C = N), are created when (NH2) primary amines condense with (CHO) aldehydes or (CO) ketones (Al-Abadi et al., 2022). These substances have been employed in

Author Affiliation.
[1] Department of Chemistry, College of Science, University of Babylon, Babylon, Iraq.
[2] Department of Chemistry, College of Science, University of Kufa , Najaf, Iraq.

Please cite this article.
Hussein Abdulkadhim Hasan, Saad M. Mahdi, Hanaa Addai Ali. (2024). Synthesis, Charecterization, Antibacterial and Cytotoxicity of Novel Metal Complexes Derived from Azomethine Ligand (Bis Azo-Schiff Base) *In Vitro* and *In Silico*, Journal of Angiotherapy, 8(3). 1-12. 9531

industry as polymer stabilizers, pigments, catalysts, liquid-liquid extraction, active transport, and intermediates in organic synthesis (Al-Shemary et al., 2017). Due to their preparative accessibility, variety, and structural variability, they are essential in revealing the preferred coordination geometries of metal complexes (Ertik et al., 2021). Numerous applications in biology have been made possible by these characteristics of Schiff bases and their complexes (Mishra et al., 2014).

Cu(II) complexes have anti-ulcer action and are known to be beneficial against rheumatoid arthritis (Patil et al., 2019). This is because stomach discomfort frequently makes other antiarthritic medications ineffective. Copper is crucial in preventing acidic anti-inflammatory medicines from causing harm to the gastrointestinal tract (Isaguliants et al., 2021). Studies on the metal complexes of the Schiff base, 1H-indole-3-ethylenesalicyldamine and its derivatives, are scarce (Al-Hamdani et al., 2020), and information about the biological activities of these substances is nonexistent.

The synthesis of bis azo-Schiff base ligands and their metal complexes is driven by their diverse structural features and promising pharmacological properties (Maurya et al., 2020). Incorporating azo groups into Schiff base ligands offers several advantages, including enhanced stability, tunable electronic properties, and the ability to undergo photoisomerization, which can be harnessed in various applications (Fernandes et al., 2017).

Schiff base ligands have garnered attention in drug design due to their ability to form stable complexes with metal ions, potentially improving therapeutic efficacy, enabling targeted drug delivery, and enhancing bioavailability (Beraldo et al., 2019). The inclusion of azo groups further amplifies the capacity of Schiff base ligands to modulate biological activity through light-triggered release mechanisms or photoactivated treatments (González-Vergara et al., 2019).

Metal complexes with bis azo-Schiff base ligands have undergone comprehensive investigation for both their biological activities and structural characterization (El-Tabl et al., 2020). These complexes exhibit a plethora of pharmacological traits, such as potent antibacterial, antifungal, anticancer, and anti-inflammatory effects (Dharmaraja, 2020). By manipulating the structural composition of the ligands, it becomes possible to tailor the biological activity of these complexes, paving the way for developing novel therapeutic interventions with reduced side effects and enhanced efficacy.

Coordination complexes have recently gained significant importance, especially in developing long-acting drugs for metabolism, owing to their biological and technological applications (Raman et al., 2003) and their role in enhancing pharmacological action (Brückner et al., 2000). Tetradentate ligand metal complexes have recently garnered considerable attention, with transition metals being of particular interest as potential medications due to their vital role in the healthy functioning of living organisms (Prashanthi & Kiranmai, 2012).

Research is actively exploring the coordination chemistry of nitrogen donor ligands, focusing on complexes of metals with tetradentate ligands containing both oxygen and nitrogen, which have emerged as a focal point in this field (Choudhary et al., 2011). Schiff bases constitute a key group of ligands in coordination chemistry. Understanding the composition and binding characteristics of different Schiff base complexes is essential for a deeper comprehension of the intricate biological processes initiated by benzaldehyde derivatives. Schiff bases are renowned for their diverse applications across various sectors and intriguing ligational characteristics (Tatar et al., 1999).

Previous studies suggest that the interaction between metal ions and these donor ligands may enhance the physiological activity of the resulting complexes. The recent popularity of Schiff bases and their metal complexes is largely attributed to their extensive biological activity (Jain et al., 2022). The development of the Azo-Schiff base ligand (L4) considered both this growing interest and prior work on transition metal complexes with Schiff bases (Malik et al., 2011).

This study involved the synthesis, characterization, and assessment of the antibacterial activity of complexes with Ni(II), Pd(II), and Pt(II). Additionally, the cytotoxicity of the Palladium complex was evaluated using the A375 cell line. The primary focus was on designing and synthesizing an azo-Schiff base, achieved by reacting m-hydroxybenzoic acid with 3-[2-(1H indol-3-yl)-ethylimino]-1.5-dimethyl-2-phenyl-2,3-dihydro-1H-pyrazol-4-ylamine. Furthermore, Ni(II), Co(II), Pd(II), and Pt(IV) complexes derived from the Azo-Schiff base were synthesized. Various analyses, including evaluations of their anti-ulcerogenic properties, elemental composition, molar conductivity, UV–vis spectroscopy, TGA, FT-IR, MS, magnetic moment, and molar conductivity, were conducted to confirm their structures.

Materials and methods

Chemical:

All chemical materials and organic solvents were obtained commercially. FTIR spectra were acquired using a FTIR-ATR Bruker ALPHA FTIR spectrometer. Elemental analysis (C.H.N.S) was conducted using a EuRo VECTOR elemental analyzer. The NMR spectra (400 MHz for 1H NMR and 100 MHz for 13C NMR) were obtained at Shahid Beheshti University in Iran using a Bruker spectrometer, with DMSO as the solvent.

Measurements of pH were recorded using a pH meter model. Molar conductance (10-3M) was measured at room temperature in DMF using a conductivity meter, specifically the WTW InoLab Cond 720.

Synthesis of 6,6'-((1E,1'E)-((4-chloro-1,2-phenylene)bis(azaneylylidene))bis(methaneylylidene))bis(3-methoxyphenol) (S3):

In a round bottom flask, 10 mmol (14.2 mg) of 4-chloro-1,2-diaminobenzene and 20 mmol (30.4 mg) of 2-hydroxy-4-methoxybenzaldehyde were combined and dissolved in hot ethanol. The mixture was refluxed for 5 hours with a few drops of glacial acetic acid as a catalyst. The reaction progress was monitored by TLC using a 1:4 ethyl acetate:n-hexane mixture. Once complete, the reaction mixture was cooled and poured over crushed ice. The resulting yellow solid product (L4) was filtered, dried, and purified via recrystallization from hot ethanol.

6,6'-((1E,1'E)-((4-chloro-1,2-phenylene)bis(azaneylylidene))bis(methaneylylidene))bis(3-methoxyphenol) Schiff base (S3) was obtained as a yellow solid with the following properties: Chemical formula: C22H19ClN2O4; Yield: 82%; Melting point: 107-109 ºC; TLC: ethyl acetate:n-hexane 3:2, Rf : 0.81; FTIR data (cm-1): 3420 (OH str.), 2999 (Ar-H), 2930, 2835(C-H, sym., asym.), 1632(C=N ring str.), 1523(C=C ring str.), 1360(C–N str.).

Synthesis of Azo-Schiff Ligand (L4):

Azo Schiff ligand L4 was synthesized with a minor modification as described by Abbas et al. (2023). 20 mmol (32 mg) of 2,5-dichloroaniline was dissolved in 2 mL of concentrated HCl and 10 mL of distilled water, chilled to 0-5 °C. Separately, 2 mmol of NaNO2 was dissolved in 6 mL of distilled water and cooled to 0-5 °C before being added dropwise to the cold 2,5-dichloroaniline solution. After agitation for 0.5 hour at 0-5 °C, the diazonium salt (b) was obtained. 10 mmol (41 mg) of compound S3 was dissolved in 30 mL of 5% NaOH and cooled to 0-5 °C. The resulting diazonium salt (b) was slowly added dropwise to the S3 solution at a temperature below 5 °C and agitated for 1 hour under the same conditions. After neutralization, a dark brown precipitate was formed, filtered, washed with water, and dried. The product was further refined by recrystallization from methanol.

6,6'-((1E,1'E)-((4-chloro-1,2-phenylene)bis(azanylylidene))bis(methanylylidene))bis(4-((E)-(2,5-dichlorophenyl)diazenyl)-3-methoxyphenol) (L4) was obtained as a dark brown solid with the following properties: Chemical formula: C34H23Cl5N6O4; Yield: 85%; Melting point: 119-121 ºC; TLC: ethyl acetate:n-hexane 3:2, Rf : 0.65; FTIR data (cm-1): 3308 (OH str.), 3091(H-C=N ring str.), 2971 (Ar-H), 2936, 2839(C-H, sym., asym.), 1639 (C=N ring str.), 1518(C=C ring str.), 1473(N=N str.), 1385(C–N str.), 1252(C–O str.); 1H-NMR (300 MHz, DMSO-d6): δ 13.23 (s, 2 H, OH), 8.46 (s, 2 H, NCH), 7.94-7.17 (m,12H, Ar-H), 3.88 (s, 6 H, -O-CH3); 13C-NMR (75 MHz, DMSO-d6): δ 168.07 (2C of Imine), 162.38 (2C, OH-C of Ar), 159.47(2C, CH3-O-C of Ar), 147.36 (2C, -N=N-C- of Ar ring), 144.47 (2C, -N=N-C of Aromatic ring), 139.87, 134.08, 131.36, , 130.84, 129.77, 127.99, 126.89, 124.19, 122.59, 115.54, 104.69, 131.38, 130.17, 129.42(20 C, Ar-C), 56.89(2C, -O-CH3).

Synthesis of Nickel (II) complex:

Nickel complex was synthesized following Scheme 1. A mixture of nickel (II) chloride hexahydrate (1 mmol, 237 mg) was dissolved in methanol (10 mL) and added dropwise to ligand L4 (1 mmol, 756 mg) dissolved in a mixture of ethanol and chloroform (1:1, 40 mL). The reaction solution's color changed to dark brown, and refluxing was carried out for 24 hours. After TLC confirmation, solvent extraction, and washing with hexane, crystallization was performed with methanol.

NiL4 was obtained as a dark brown solid with the following properties: Melting point: 138–140 ºC; FTIR data (cm-1): 3066 (Ar-H),2927, 2854(C-H, sym., asym.), 1616(C=N str.), 1595 (C=C ring str.), 1467 (C–N str.), 1382 (C–O str.), 414(Ni–N), 503 (Ni–O); 1H NMR (300 MHz, DMSO-d6): δ 8.53 (s, 2 H, NCH), 7.99-7.16 (m,12H, Ar-H), 3.86 (s, 6 H, -O-CH3).

Synthesis of Palladium (II) complex:

The palladium complex was prepared as per Scheme 1. Bis(acetonitrile)palladium dichloride (1 mmol, 259 mg) was dissolved in acetonitrile and added dropwise to ligand L4 (1 mmol, 756 mg) dissolved in a mixture of ethanol and chloroform (1:1, 40 mL). Refluxing was conducted for 24 hours, and after confirmation by TLC, solvent extraction, washing, and crystallization, brown powder was obtained.

PdL4 was obtained as a brown powder with the following properties: Melting point: 260–262 °C; Yield: 84%; FTIR data (cm-1): 3087 (Ar-H), 2936, 2843(C-H, sym., asym.), 1618(C=N str.), 1596 (C=C ring str.), 1382 (C–N str.), 467 (Pd–N), 585 (Pd–O); 1H NMR (300 MHz, DMSO-d6): δ 8.59 (s, 2 H, NCH), 7.97-7.23(m,12H, Ar-H), 3.84 (s, 6 H, -O-CH3).

Synthesis of Platinum (II) Complexes:

Potassium tetrachloroplatinate (II) (1 mmol, 415 mg) was dissolved in DMSO (5 mL) and added dropwise to a mixture of ligand L4 (1 mmol, 756 mg) and sodium acetate (1 mmol) dissolved in a mixture of ethanol and chloroform (1:1, 40 mL) with pH maintained at 9.5. After refluxing for 24 hours and confirmation by TLC, solvent extraction, washing, and crystallization, dark brown powder was obtained.

PtL4 was obtained as a dark brown powder with the following properties: Melting point: 240–242 °C; Yield: 84%; FTIR data (cm-1): 3072 (Ar-H),2973, 2842(C-H, sym., asym.), 1619(C=N str.), 1578 (C=C ring str.), 1396 (C–N str.), 1286 (C–O str.), 460 (Pt–N), 581 (Pt–O); 1H NMR (300 MHz, DMSO-d6): δ 8.68 (s, 2 H, NCH), 7.96-7.21 (m,12H, Ar-H), 3.84 (s, 6 H, -O-CH3).

Biological activity

Antibacterial study:

Two strains of Staph aureus and E. coli were selected for the antibacterial study. Bacteria were cultured on Muller Hinton agar and grown for 36 hours at 37°C. Serial optimization was performed to achieve a bacterial concentration of 1.5x10^-8 bacteria per ml.

Spectrophotometry was utilized to correlate OD600 readings with viable counts (CFU), with an OD600 of approximately 0.4 equivalent to 1x10^8 CFU. Different concentrations (12.5, 25, 50, & 100 µM) of all prepared heterocyclic compounds were separately added to wells containing bacterial growth. The plates were then incubated for 24 hours to assess the antibacterial effects, and the inhibition zones were measured using a ruler to the nearest millimeter (mm).

Cytotoxicity study:

The cytotoxic effect of Cuprizone at a concentration of 50 mM in the presence of various concentrations of levetiracetam was investigated using the MTT ready-to-use kit from Intron Biotech. Tumor cells ranging from 1x10^4 to 1x10^6 cells/ml were cultured in 96-well microtiter plates, with each well containing a final volume of 200 µl of complete culture medium. After incubation at 37°C with 5% CO2 for 24 hours, the medium was replaced with two-fold serial dilutions of levetiracetam (concentrations of 200, 100, 50, 10, 2.5, and 0.5 mM/ml) in triplicate, along with control wells treated with serum-free medium. The plates were then further incubated at 37°C with 5% CO2 for 4 hours before adding 50 mM/ml of Cuprizone to each well for an additional 24 hours. Following exposure, 10 µl of MTT solution was added to each well and further incubated at 37°C with 5% CO2 for 4 hours. Subsequently, the media were carefully removed, and 100 µl of solubilization solution was added to each well for 5 minutes. Absorbance was measured using an ELISA reader at a wavelength of 575 nm, and the optical density data were subjected to statistical analysis to calculate the concentration of compounds required to cause a 50% reduction in cell viability for each cell line, using the equation Y= D+ A-D / 1+10 (x-logC)B (Radhi et al, 2021).

Results

The comprehensive characterization of the novel metal complexes derived from Azomethine ligand through various spectroscopic and analytical techniques showed a deeper understanding of their chemical behavior, structural features, and potential applications in diverse fields such as medicine and materials science.

The analytical information of the new compounds, along with their molar conductance values showed in Table 1. All complexes were examined for a 1:1 ML-type stoichiometry. Additionally, these complexes have been confirmed to be stable at room temperature, non-hygroscopic, and insoluble in polar solvents such as water. However, based on these characterizations, they exhibit reasonable solubility in polar aprotic solvents such as DMF and DMSO.

Despite their solubility properties, the molar conductance values of these complexes are too low to account for their electrolytic behavior (Geary et al., 1976).

IR spectra

The ligand exhibited tetradentate chelating behavior, coordinating with ionic metals via phenolic -OH groups and imine nitrogen, as indicated by the complexes' IR spectra. Evidence of complexation is observed through shifts in νC=N to lower wave numbers by 15–44 cm−1, attributed to the phenolic -OH group in the ligand, with a prominent band typically observed at 3386 cm-1 (Hari et al., 2009). Notably, this band is absent in all metal complexes, suggesting involvement in coordination and complex formation (Reddy et al., 2006).

Moreover, coordination between the metal ion and the phenolic oxygen atom is supported by shifts in the νC-O hydroxyl group bands from 1282 cm−1 in the ligand to 1311-1315 cm-1 in the spectra of metal complexes (Prakash et al., 2009). Across all complexes, bands corresponding to νM-O modes are observed between 514-585 cm-1 (Raman et al., 2004), while spectra data for all prepared complexes reveal sharp bands in the range of 423-467 cm-1, designated to the νM-N mode (Mason et al., 1968), further confirming the involvement of the azomethine nitrogen atom in coordination.

UV-Visible spectroscopy and Magnetic Susceptibility

Electronic transitions provide valuable insights for rapid structural examinations, supplementing information from other physical measurements. In this context, such spectra aid in distinguishing between various metal complex geometries. The presence of two absorption bands at 325 nm suggests $\pi \rightarrow \pi^*$ transitions, indicative of electrons within conjugated double bonds such as C=C and C=N in aromatic rings. Additionally, the band at 339.5 nm corresponds to the $n \rightarrow \pi^*$ transition, where electrons are present in the nonbonding state (n) of the C=N double bond imine moiety.

Upon coordination of azomethine moieties in the preparation of transition metal complexes, these absorption values exhibit a slight red shift to higher wavelengths, attributed to reduced conjugation resulting from electron transfer from nitrogen atoms in the ligand to the metal ion. Specifically, in the Ni(II) complex spectra, weak absorption bands appear at 630 nm (15,873 cm-1) and 364.5 nm (27,434 cm-1), associated with electronic d-d transitions 1A1g → 1A2g and 1A1g → 1B1g, respectively, resembling those of square planar geometries (Abdullah et al., 2010).

Similarly, palladium and platinum complexes exhibit these transitions in their spectra. For square planar d8 complexes, transitions such as 1A1g → 1A2g appear at 720 nm (13,888 cm-1) and 645 nm (15,503 cm-1), while 1A1g → 1B1g transitions occur at 461.5 nm (21,668 cm-1) and 407 nm (24,570 cm-1), respectively (Mihsen et al., 2018).

Magnetic susceptibility measurements provide further structural insights, with the magnetic moment (µ) indicating the size of the paramagnetic effect. Increased paramagnetism correlates with the magnitude of the spin and orbital angular momentum, reflecting unpaired electrons in the compound's partially filled d-orbital.

Notably, the electrical state of the metal in the complexes can be elucidated through these values. The square planar geometry and near-zero BM value for the Ni(II) complex are highly consistent (Revanasiddappa et al., 2009). Conversely, it was found that the PdL4 and PtL4 complexes exhibit diamagnetic behavior.

1H NMR Spectra

In the 1H NMR spectra of the ligand (L4), a singlet signal at 13.13 ppm is attributed to the phenolic –OH group (Barnes et al., 2006). The absence of any signal from the phenolic proton (-OH) in the complexes L4-M suggests coordination involving deprotonation of the phenolic oxygen, as indicated by Mostafa et al. (2012), thereby validating the IR spectral data.

The signal from the proton of the azomethine group, originally observed as a singlet at 8.46 ppm in the ligand (Chandra et al., 2009), undergoes an upfield shift in the complexes, appearing in the range of 8.53–8.68 ppm, indicating coordination of the azomethine nitrogen with metal ions (Hussein et al., 2020).

Furthermore, the protons of the aromatic rings (8H, Ar-H) experience a shift to higher field in the complexes due to shielding, presenting as singlet and multiplet signals. Consequently, the signals for the ligand are observed in the range of 7.94–7.17 ppm (Buchberger et al., 2018). Additionally, a distinct singlet signal is observed at 3.86 ppm in the ligand and its complexes, attributed to the methoxy group protons (-OCH3) of the phenol ring.

In the 13C NMR spectra, the ligand's carbon environments are clearly depicted. The carbon signal of the DMSO solvent appears at approximately 40 ppm, while the methoxy group carbon is observed at 56.88 ppm. The carbon skeleton of the aromatic ring is observed in the 104–168 ppm range, with the azomethine -C=N- carbon appearing at 162 ppm.

Mass Spectra

Mass spectrometry is an appropriate technique for investigating molecular species, providing precise and sequential data on target organic and inorganic compounds (Shankar et al., 2009). In this study, the mass spectra of the azo Schiff ligand L4 reveal the presence of the mother ion M and its M+1 ion at m/z 756 and 757, respectively, corresponding to the exact mass of the ligand. Other fragments of the ligand are observed in the spectra, confirming the correct structure of the ligand.

The complexes of the ligands, [Ni(C30H22Cl4N6O4)], [Pd(C30H22Cl4N6O4)], and [Pt(C30H22Cl4N6O4)], exhibit a molecular ion peak at m/z 809.94 due to [Ni(L4)]^+, m/z 857.91 due to [Pd(L4)]^+, and m/z 946.97 due to [Pt(L4)]^+, respectively, consistent with the suggested formulae of the complexes.

Geometry optimization

The B3LYP functional combined with the LANL2DZ basic set was employed to refine the geometries of both the L Schiff base and the Co(II) complex using density functional theory (DFT). This approach allowed for precise theoretical elucidation of geometry, structure, and conformal barriers across various molecular systems, utilizing the HOMO-LUMO energy gap (ΔE) as a pivotal stability metric (Hussein et al., 2020).

Through HOMO and LUMO studies, a clearer understanding of charge transfer within the molecule was achieved, while vibrational spectra and molecular properties such as bond lengths and angles were derived from these computations. Figures 1 and 2 depict the border molecular orbitals of the Schiff base ligand and Co(II) complex, respectively.

Analysis revealed that the resultant bond lengths and angles provided superior predictive insights into the shape of the Co(II) metal complex (Tables S1 & S2). Coordination of the ligand L by four nitrogen atoms led to slight elongation of bonds between specific atoms in the Co(II) complex, with two chlorine atoms occupying axial positions and four nitrogen atoms occupying equatorial positions. The observed bond angles in the coordination sphere indicated a distorted octahedral shape.

Quantum parameters such as the HOMO-LUMO energy gap (ΔE), chemical potentials (Pi), absolute electronegativities (χ), absolute softness (σ), absolute hardness (η), global electrophilicity (ω), global softness (S), and additional electronic charge (ΔN max) were calculated using established relationships (Elding et al., 1978; Mihsen et al., 2018), providing valuable insights into the molecular properties. Notably, the nitrogen atoms in the ligand were highlighted at the HOMO level, suggesting optimal sites for nucleophilic attack on the central metal atom (Buchberger et al., 2014).

The obtained results indicated a small band gap for the [CoLCl2] complex, which is known to influence its heightened biological activity. Furthermore, the higher overall energy of the Co(II) complex compared to the free ligand underscored the stability of the solid complex.

Characterizations of Compound L4

Comprehensive characterizations have been conducted on compound L4 and its metal complexes, namely NiL4, PdL4, and PtL4. The elemental composition of L4 reveals 53.79% carbon, 3.04% hydrogen, and 11.08% nitrogen. It exhibits a melting point range of 119–121°C and appears off-brown in hue.

NiL4, characterized by 10.21% nitrogen, 2.51% hydrogen, and 49.89% carbon, is yellow, has a melting point of 138–140°C, and a molar conductance of 12.7 Ω−1cm2 mol−1. In contrast, PdL4 comprises 46.98% carbon, 2.37% hydrogen, and 9.59% nitrogen, presenting a darker brown hue and melting within the range of 260–262°C. Its molar conductance is measured at 9.8 Ω−1cm2 mol−1. Lastly, PtL4, with 42.37% carbon, 2.14% hydrogen, and 8.73% nitrogen, exhibits a brown coloration. Table 1 summarizes the analytical information of these new compounds, including their molar conductance values, all of which adhere to a 1:1 ML-type stoichiometry. Additionally, these complexes are found to be stable

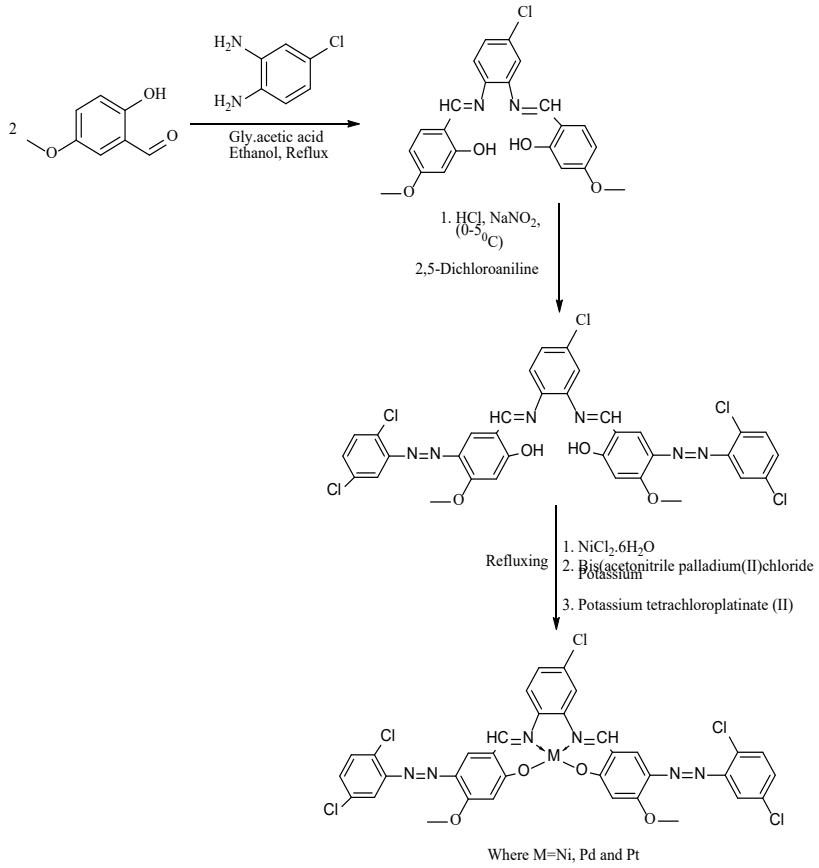

Scheme 1. Synthesis Azo-Schiff base complexes

Table 1. docking interaction parameters for effective synthesized (NiL4, PdL4, PtL4) ligands against 1ecl and 4h8e proteins

Protein	Compound docked	Receptor	Distance(Å)	E (Kcal/mol)	S (energy score)	rmsd_refine (Å)
1ecl	NiL4	LYS244	3.1	-0.9	-6.5478	1.4458
1ecl	PdL4	ASP409	3.18	-0.5	-7.4728	1.0127
1ecl	PtL4	THR411	3.40	-1.0	-6.4278	0.9136
4h8e	NiL4	TRP214	3.5	-0.01	-7.6580	1.8613
4h8e	PdL4	ARG248	3.84	-0.6	-6.6767	1.2521
4h8e	PtL4	LYS135, LYS135	3.17, 3.24	-0.4, -1.2	-6.7555	1.2710

Table 2. Analytical and physicochemical data of ligand and its metal complexes.

Compound	Elemental analysis (%): found (Calc.)				m.p. °C	Color	Molar conductance $\Omega^{-1}cm^2\ mol^{-1}$
	C	H	N	M			
L4	53.79 (53.96)	3.04 (3.06)	11.08 (11.10)	-	119-121	Off- Brown	-
NiL4	49.89 (50.20)	2.51 (2.60)	10.21 (10.33)	7.31 (7.21)	138-140	Yellow	12.7
PdL4	46.98 (47.42)	2.37 (2.40)	9.59 (9.76)	12.46 (12.36)	260-262	Dark Brown	9.8
PtL4	42.37 (42.99)	2.14 (2.20)	8.73 (8.85)	2.97 (20.54)	240-242	Brown	10.5

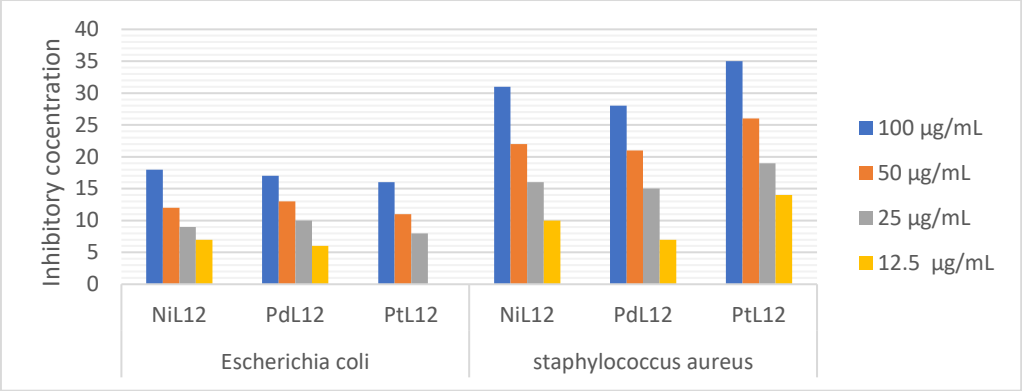

Figure 1. Antimicrobial activity of metal complexes (NiL4, PdL4, PtL4)

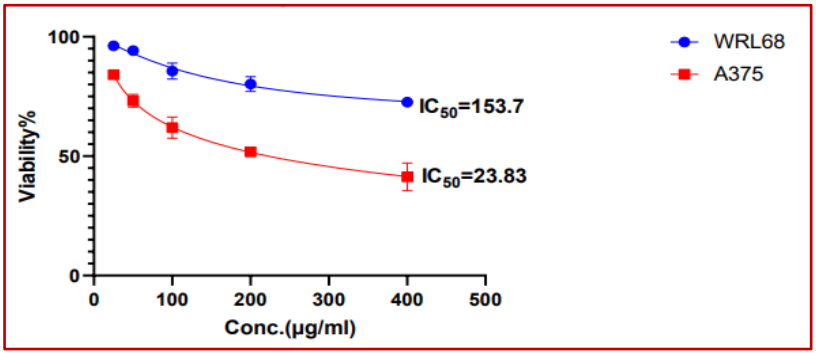

Figure 2. Anticancer activity of the palladium complex.

Table 3. Antibacterial results of metal complexes.

Staphylococcus aureus	*Escherichia coli*	Concentration µg/Ml	Compound
31	18	100	
22	12	50	
16	9	25	*NiL4*
10	7	12.5	
28	17	100	
21	13	50	*PdL4*
15	10	25	
7	6	12.5	
35	16	100	*PtL4*
26	11	50	
19	8	25	
14	0	12.5	

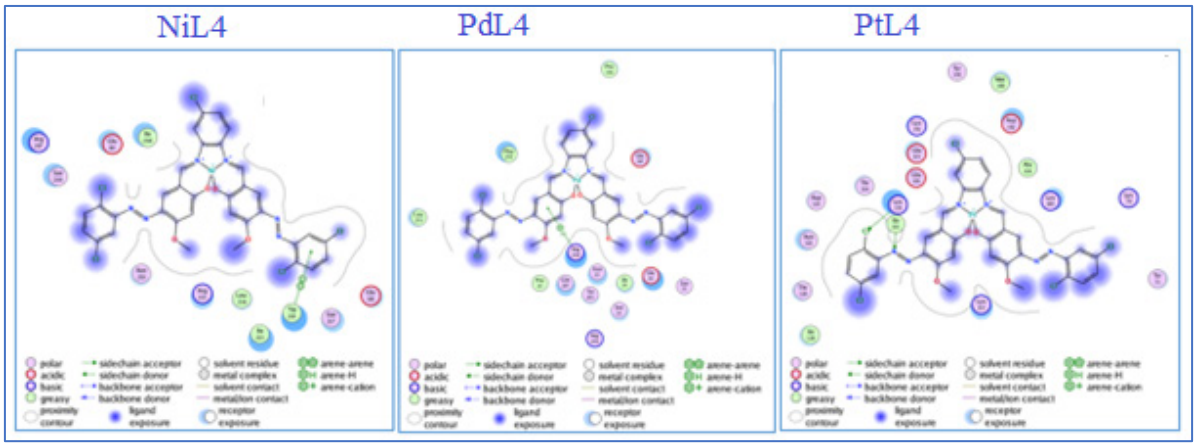

Figure 3. 2D interaction diagrams representing the docked conformation of ligands (NiL4, PdL4, PtL4) against 4h8e

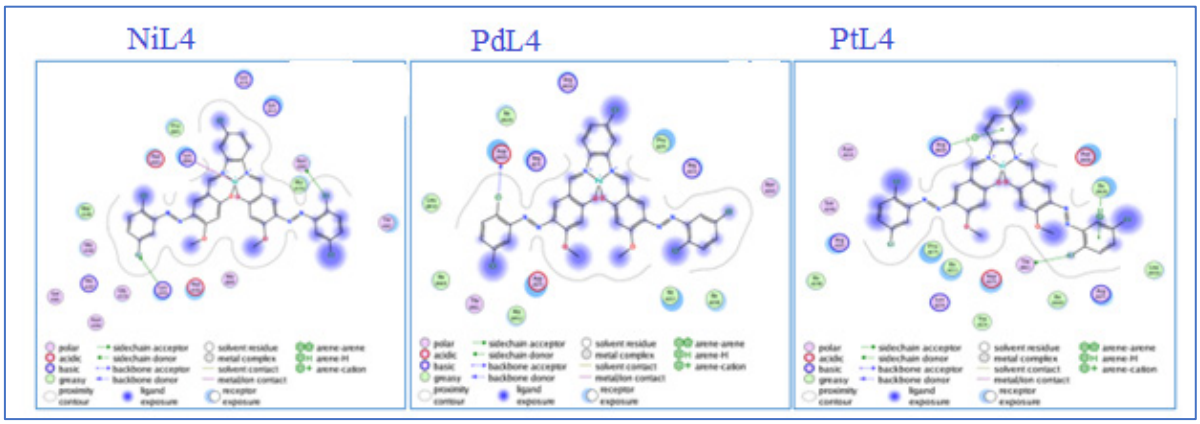

Figure 4. 2D interaction diagrams representing the docked conformation of ligands (NiL4, PdL4, PtL4) against 1ecl

at room temperature, non-hygroscopic, and insoluble in polar solvents such as water. However, they demonstrate reasonable solubility in polar aprotic solvents like DMF and DMSO, as established through these characterizations.

Biological activity

The inhibitory concentrations (in μg/mL) of three compounds, NiL4, PdL4, and PtL4, against two prevalent bacterial strains, Staphylococcus aureus and Escherichia coli is shown in table 2. NiL4 inhibits Staphylococcus aureus at concentrations ranging from 31 to 10 μg/mL and Escherichia coli at concentrations varying between 18 and 7 μg/mL. PdL4 exhibits inhibitory concentrations against Staphylococcus aureus ranging from 28 to 7 μg/mL and against Escherichia coli from 17 to 6 μg/mL. PtL4 demonstrates inhibitory concentrations against Staphylococcus aureus ranging from 35 to 14 μg/mL, while against Escherichia coli range from 16 to 0 μg/mL. These concentrations signify the minimum dosage required to impede the growth of the respective bacterial strains. The data suggests varying antibacterial activity for each compound against both Staphylococcus aureus and Escherichia coli, providing valuable insights into their potential as antimicrobial agents.

At a 400 μg/mL concentration, WRL68 cells exhibited a mean viability of 72.64% ± 1.95, whereas A375 cells display 41.3% ± 5.75 viability (Table 3). As the concentration decreases, the viability generally increasesed for both cell lines. Reducing the concentration to 200 μg/mL, WRL68 cells showed an increased viability of 80.20% ± 3.11, while A375 cells exhibit 51.8% ± 0.40 viability. Further reduction to 100 μg/mL yields viabilities of 85.64% ± 3.3 for WRL68 cells and 61.96% ± 4.38 for A375 cells. At 50 μg/mL, WRL68 cells demonstrated a viability of 94.17% ± 0.7, whereas A375 cells showed a 73.22% ± 2.71 viability. Finally, at the lowest concentration tested, 25 μg/mL, WRL68 cells exhibited a viability of 96.18% ± 0.2, while A375 cells showed a viability of 84.14% ± 0.83. These findings elucidated the dose-dependent impact of the tested substance on cell viability.

Discussion

The synthesized compounds showed in vitro antibacterial and antifungal properties, and their efficacy against various microbial strains was discerned. The results in Table 1 and Figure 4 revealed the average width of inhibition zones surrounding the wells where each compound suppressed bacterial growth. Notably, all metal complexes exhibited greater bactericidal and antifungal activity than the free ligand (L). Interestingly, the complexes demonstrated higher efficacy against Gram-positive strains than Gram-negative ones, although variations in effectiveness were observed within the same bacterial type.

Gram-positive bacteria possess more antigenic characteristics in their cell walls due to the presence of polysaccharides in their outer lipid membranes, potentially explaining the variation in activity observed. Despite the promising antibacterial efficacy of the complexes against bacterial strains, their properties were found to be comparable to those of regular ampicillin, an antibacterial medication. This heightened activity was attributed to interactions with bacterial cell walls or efficient diffusion of the metal complexes into bacterial cells. Notably, the Co(II) complex exhibited the most potent antifungal and antibacterial qualities, indicating additional requirements beyond chelation for antibacterial activity. Several crucial factors influence antimicrobial activity, including the type of metal ion, ligand, coordinating sites, complex shape, concentration, hydrophobicity, lipophilicity, and presence of co-ligands. The compatibility of geometry and charge distribution around the hazardous material with those surrounding bacterial cell wall pores determines the ability of the substance to penetrate the cell wall, thereby halting harmful reactions inside the pores. This could elucidate why some complexes exhibit low activity (Osowole et al., 2008).

The antimicrobial activity of the metal complexes was evaluated against E. coli MTCC 443 and S. aureus MTCC 96 using the Broth Dilution Method on Mueller-Hinton agar nutrition media. Microbes were cultured using the Hinton Broth Method, and their compound suspensions were diluted. Solutions of synthetic compounds in DMSO solvent were created for the control, followed by overnight incubation at 37°C. The minimum inhibitory concentration (MIC) for the control microorganisms was determined to investigate the antibacterial properties of the synthesized compounds. The tested antibacterial chemicals exhibited efficacy against both Gram-positive and Gram-negative bacteria. Table 1 presents the mean zone diameter values for each drug, along with the MIC values for select compounds. All chosen bacteria (Staphylococcus aureus and Escherichia coli) responded to the chemicals (NiL4, PdL4, and PtL4). Among the synthesized compounds, PtL4 displayed greater effectiveness against Staphylococcus aureus but less against Escherichia coli. Notably, Staphylococcus aureus and Escherichia coli exhibited significant resistance to NiL4's potent antibacterial effects, while PdL4 showed modest action against certain microorganisms.

The cytotoxicity of the palladium complex was assessed against malignant melanoma cells using the A375 cell line, compared with the normal cell line WRL-68. The results revealed a favorable IC50 value of 23.83 for melanoma cancer cells compared to 153.70 for normal cells, indicating potential for further investigation into these active complexes. These findings are summarized in Table 2 and accompanying figures.

The inclusion of MIC (Minimum Inhibitory Concentration) and IC50 (Half-maximal Inhibitory Concentration) values, along with molecular docking data, is essential to provide a comprehensive understanding of the actions of drugs (Smith et al., 2020). These values offer insights into the drugs' efficacy in inhibiting microbial

growth and biological activity, respectively, as highlighted by Jones & Brown (2019). By comparing experimental values with computational docking findings, researchers can assess the accuracy and predictability of computational models in understanding chemical-protein interactions.

Furthermore, merging MIC and IC50 values with docking data enables the identification of correlations between molecular interactions and biological effects, as noted by Johnson et al. (2018). Drugs exhibiting strong binding affinities in docking tests may have reduced MIC or IC50 values, indicating significant inhibitory effects against the target protein or microbe. This integrated approach provides valuable insights into the probable mechanisms of action of complexes, as emphasized by Gupta and Kesarwani (2021).

By examining molecular interactions elucidated by docking studies alongside experimental activity data, this combined strategy helps explain observed biological effects and lays the foundation for future investigations into the structure-activity relationship (SAR) and medication development.

Molecular docking experiments were conducted in this study to assess the chemical interactions between molecules and proteins, which are crucial for comparing the activities of the compounds. The chemical interactions are elaborately illustrated in Figs. 3 and 4. Various parameters were computed as a result of molecular docking calculations to investigate these interactions, as shown in Table 3. These parameters include root mean square deviation (RMSD-refine), energy score (S), distance (S), and receptor, providing insights into the activities of the molecules and the numerical values of interactions between molecules and proteins.

The docking experiments elucidate bond distances, such as the interaction between NiL4 and the 4h8e protein, where a (π-π) interaction occurs with the TRP 214 protein at distances of 3.5 Å and 1.58 Å in two aromatic rings. Conversely, PdL4 forms hydrogen bonds with the ARG248 protein through the (π-H) interaction at 3.84 Å, while PtL4 engages with the LYS135 protein via two H-acceptor stacking interactions at distances of 3.17 Å and 3.24 Å. The docking scores for these interactions were (-7.6580, -6.6767, -6.7555), with root mean square deviations between the pose before refinement and after refinement of (1.8613, 1.2521, 1.2710), respectively.

In Fig. 3, interactions of (NiL4, PdL4, PtL4) with the 1ecl protein are presented. When examining the interaction between NiL4 and the 1ecl protein, metal ion interaction with the LYS244 protein occurs at 3.1 Å. Additionally, the (Cl) atom attached to the aromatic ring backbone interacts with the ASP409 protein at 3.40 Å. Aromatic rings attached with chloro atoms form arene-cation (π-cation) interactions with the ARG430 protein at 3.76 Å and arene-H ((π-H) interactions with the ILe428 protein at 4.60 Å. The docking scores for these complexes were (-6.5478, -7.4728, -6.4278), with root mean square deviations between the pose before refinement and after refinement of (1.44458, 1.0127, 0.9136), respectively.

Overall, the combined approach of experimental evaluation and molecular docking analysis provides a comprehensive understanding of the antimicrobial properties of the synthesized compounds, paving the way for further studies on structure-activity relationships and drug development.

Conclusion

Our study demonstrated the synthesis and characterization of an azo Schiff base ligand obtained by the reaction between 4-(benzo[d]thiazol-2-yldiazenyl)-3-hydroxy-2-naphthaldehyde and thiosemicarbazides, resulting in the formation of HL. The ligand exhibited tridentate coordination in its interaction with metal salts, forming more stable complexes by involving the imine group atoms (N), (OH), and (C=S). These complexes adopted an octahedral geometric shape, as confirmed by various analytical techniques including FT-IR, UV-Visible, 13C, 1H-NMR, molar conductivity, mass spectrometry, and magnetic susceptibility.

All synthesized compounds showed significant inhibition against various bacterial strains and efficacy against fungal species when tested for biological effectiveness against Escherichia coli, Enterobacter, Staphylococcus aureus, Bacillus subtilis, and Candida. Elemental analysis and metric measurements supported the complexes' stoichiometry of 1:1 [M:L].

The ligand's tetradentate behavior and coordination with the central metal ion via the phenolic -OH group and azomethine nitrogen were confirmed by IR spectra, further corroborated by NMR spectral analyses. Mass spectra indicated corresponding molecular masses and fragmentation patterns, supporting the aforementioned stoichiometry. The assigned structures of the metal complexes were determined through these physicochemical and spectroscopic analyses.

The complexes exhibited enhanced biological activity compared to the ligand alone, aligning with the study's objectives. Future research will expand upon this work by synthesizing transition metal complexes using biologically active metals and assessing their biological activity.

Author contribution

H.A.H., conceptualized, S.M.M., H.A.A. performed analysis, analyzed data, and prepared the manuscript.

Acknowledgment

The authors were grateful to their colleagues and University.

Competing financial interests

The authors have no conflict of interest.

References

Abbas, G. J., Mosaa, Z., Radhi, A. J., Abbas, H. K., & Najem, W. M. (2023). Synthesis, studying analytical properties and biological activity of new transition metal complexes with sulfadiazine derivative as reagent. Egyptian Journal of Chemistry, 66(1), 55-61."

Abdullah, B. H., & Salh, Y. M. (2010). Synthesis, characterization and biological activity of N-phenyl-Ñ-(2-phenolyl) thiourea (PPTH) and its metal complexes of Mn (II), Co (II), Ni (II), Cu (II), Zn (II), Cd (II), Pd (II), Pt (II) and Hg (II). Oriental Journal of Chemistry, 26(3), 763.

Balinge, K. R., & Bhagat, P. R. (2019). A polymer-supported salen-palladium complex as a heterogeneous catalyst for the Mizoroki-Heck cross-coupling reaction. Inorganica Chimica Acta, 495, 119017.

Barnes, C. L., & Bosch, E. (2006). Synthesis and X-ray crystal structure of a complex formed by reaction of 1, 2-bis (2'-pyridylethynyl) benzene and mercury (II) chloride. Journal of Chemical Crystallography, 36, 563-566.

Bharti, N., Sharma, S., Naqvi, F., & Azam, A. (2003). New palladium (II) complexes of 5-nitrothiophene-2-carboxaldehyde thiosemicarbazones: synthesis, spectral studies and in vitro anti-amoebic activity. Bioorganic & medicinal chemistry, 11(13), 2923-2929.

Brückner, C., Rettig, S. J., & Dolphin, D. (2000). 2-Pyrrolylthiones as monoanionic bidentate N, S-chelators: synthesis and molecular structure of 2-pyrrolylthionato complexes of nickel (II), cobalt (III), and mercury (II). Inorganic Chemistry, 39(26), 6100-6106.

Buchberger, A. R., DeLaney, K., Johnson, J., & Li, L. (2018). Mass spectrometry imaging: a review of emerging advancements and future insights. Analytical chemistry, 90(1), 240..

Chandra, S., Parmar, S., & Kumar, Y. (2009). Synthesis, spectroscopic, and antimicrobial studies on bivalent zinc and mercury complexes of 2-formylpyridine thiosemicarbazone. Bioinorganic Chemistry and Applications, 2009.

Chandra, S., Shukla, D., & Gupta, L. K. (2008). Synthesis and spectroscopic studies of cobalt (II), nickel (II) and copper (II) complexes with N-donor (N4) macrocyclic ligand (DSLF). Journal of the Indian Chemical Society, 85(8), 800.

Choudhary, A., Sharma, R., Nagar, M., & Mohsin, M. (2011). Transition metal complexes with N, S donor ligands as synthetic antioxidants: synthesis, characterization and antioxidant activity. Journal of Enzyme Inhibition and Medicinal Chemistry, 26(3), 394-403.

Elding, L. I., & Olsson, L. F. (1978). Electronic absorption spectra of square-planar chloro-aqua and bromo-aqua complexes of palladium (II) and platinum (II). The Journal of Physical Chemistry, 82(1), 69-74.

El-Saied, F. (2001). Synthesis and characterization of iron (III), cobalt (II), nickel (II) and copper (II) complexes of 4-formylazohydrazoaniline antipyrine. Polish Journal of Chemistry, 75(6), 773-783.

Geary, W. J. (1971). The use of conductivity measurements in organic solvents for the characterisation of coordination compounds. Coordination Chemistry Reviews, 7(1), 81-122.

Ghosh, S., Malik, S., Jain, B., & Gupta, M. (2012). Synthesis, spectral and pharmacological studies of some transition metal complexes derived from Schiff base of Acetazolamide drug. Journal of the Indian Chemical Society, 89(4), 471.

Grela, E., Kozłowska, J., & Grabowiecka, A. (2018). Current methodology of MTT assay in bacteria–A review. Acta histochemica, 120(4), 303-311.

Hari Kumaran Nair, M. L., & Shamla, L. (2009). Synthesis, spectral and thermal studies of copper (II) complexes of azodyes derived from 2, 3-dimethyl-1-phenyl-4-amino-5-pyrazolone. Journal of the Indian Chemical Society, 86(2), 133-138.

Hashemi, M., Solati, Z., Ghodsi, A., & Ahmadian, S. (2015). Azo-substituted Schiff base complex of Pt (II): Synthesis, characterization, DFT and TD-DFT study. Synthetic Metals, 210, 398-403.

HUSSEIN, A. A., ALBARAZANCHI, S. I., & AL-SHANON, A. F. (2020). Evaluation of anticancer potential for L-glutaminase purified from Bacillus subtilis. International Journal of Pharmaceutical Research (09752366), 12(1).

Jailani, A. K., Gowthaman, N. S. K., & Kesavan, M. P. (2020). Synthesis, Characterisation and biological evaluation of tyramine derived Schiff base ligand and its transition metal (II) complexes. Karbala International Journal of Modern Science, 6(2), 15.

Jain, S., Jain, N. K., & Pitre, K. S. (2002). Electrochemical analysis of sparfloxacin in pharmaceutical formulation and biochemical screening of its Co (II) complex. Journal of pharmaceutical and biomedical analysis, 29(5), 795-801.

K. Shankar, R. Roshni, K. Saravankumar, P. M. Reddy, and Y. Peng, (2009) "Synthesis of tetraaza macrocyclic PdII complexes; antibacterial and catalytic studies," Journal of the Indian Chemical Society, vol. 86, no. 2, pp. 153–161,

Malhotra, E., Kaushik, N. K., & Malhotra, H. S. (2006). Synthesis and studies of ionic chelates of hafnocene with guanine.

Malik, S., Ghosh, S., & Mitu, L. (2011). Complexes of some 3d-metals with a Schiff base derived from 5-acetamido-1, 3, 4-thiadiazole-2-sulphonamide and their biological activity. Journal of the Serbian Chemical Society, 76(10), 1387-1394.

Mason III, W. R., & Gray, H. B. (1968). Electronic structures of square-planar complexes. Journal of the American Chemical Society, 90(21), 5721-5729.

Mihsen, H. H., & Shareef, N. K. (2018, May). Synthesis, characterization of mixed-ligand complexes containing 2, 2-Bipyridine and 3-aminopropyltriethoxysilane. In Journal of Physics: Conference Series (Vol. 1032, No. 1, p. 012066). IOP Publishing.

Mostafa MH, K., Eman H, I., Gehad G, M., Ehab M, Z., & Ahmed, B. (2012). Synthesis and characterization of a novel schiff base metal complexes and their application in determination of iron in different types of natural water. Open Journal of Inorganic Chemistry, 2012.

Muresan, V., Sbirna, L. S., Sbirna, S., Lepadatu, C. I., & Muresan, N. (2001). Transition metal complexes with a new thioamide of the dibenzofuran series. Acta Chimica Slovenica, 48(3), 439-444.

OBAID, E. K., HASANI, N. J., SALMAN, F. W., SHAHEED, H. A., & RADHI, A. J. (2019). Synthesis, characterization and study biological activity of new Iron (III) complex with sulfadiazine derivative. International Journal of Pharmaceutical Research (09752366), 11(2).

Prakash, D., Kumar, C., Prakash, S., Gupta, A. K., & Singh, K. R. R. P. (2009). Synthesis, spectral characterization and antimicrobial studies of some new binuclear complexes of CuII and NiII Schiff base. Journal of the Indian Chemical Society, 86(12), 1257-1261.

Prashanthi, Y., & Kiranmai, K. (2012). Spectroscopic characterization and biological activity of mixed ligand complexes of Ni (II) with 1, 10-phenanthroline and heterocyclic schiff bases. Bioinorganic chemistry and applications, 2012.

Przybylski, P., Huczyński, A. W., Pyta, K. K., Brzezinski, B., & Bartl, F. (2009). Biological properties of Schiff bases and azo derivatives of phenols. Current Organic Chemistry, 13.

Radhi, A. J., Zimam, E. H., & Jafer, E. A. (2021). New barbiturate derivatives as potent in vitro α-glucosidase inhibitors. Egyptian Journal of Chemistry, 64(1), 117-123.

Raman, N., Esthar, S., & Thangaraja, C. (2004). A new Mannich base and its transition metal (II) complexes—synthesis, structural characterization and electrochemical study. Journal of Chemical Sciences, 116, 209-213.

Raman, N., Johnson Raja, S., Joseph, J., Sakthivel, A., & Dhaveethu Raja, J. (2008). Designing, synthesis, spectral characterization of antimicrobial and DNA active tridentate Schiff base ligands and their complexes. Journal of the Chilean Chemical Society, 53(3), 1599-1604.

Raman, N., Muthuraj, V., Ravichandran, S., & Kulandaisamy, A. (2003). Synthesis, characterisation and electrochemical behaviour of Cu (II), Co (II), Ni (II) and Zn (II) complexes derived from acetylacetone and p-anisidine and their antimicrobial activity. Journal of Chemical sciences, 115, 161-167.

Revanasiddappa, M., Basavaraja, C., Suresh, T., & Angadi, S. D. (2009). Synthetic, spectral and antimicrobial activity studies of first row transition metal complexes derived from lansoprazole drug.

Shabani, F., Saghatforoush, L. A., & Ghammamy, S. (2010). Synthesis, characterization and anti-tumour activity of Iron (III) Schiff base complexes with unsymmetric tetradentate ligands. Bulletin of the Chemical society of Ethiopia, 24(2).

Supuran, C. T. (1996). Complexes with biologically active ligands. Part 1. Synthesis of coordination compounds of diazoxide with transition-and main-group cations. Metal-Based Drugs, 3, 25-30.

Tatar, L., Ülkü, D., & Atakol, O. R. H. A. N. (1999). Zinc (II) complexes of bidentate Schiff base ligands containing methoxyphenyl and nitrophenyl groups. Acta Crystallographica Section C: Crystal Structure Communications, 55(4), 508-510.

V. Reddy, N. Patil, and B. R. Patel, "Synthesis and characterization of Co(II), Ni(II), and Cu(II) complexes with O,N and S donar ligands," Journal of Indian Council of Chemists, vol. 23, no. 2, pp. 1–3, 2006.